



UNIVERSITY OF LEEDS

This is a repository copy of *Initiation and evolution of knickpoints and their role in cut-and-fill processes in active submarine channels*.

White Rose Research Online URL for this paper:
<https://eprints.whiterose.ac.uk/165536/>

Version: Accepted Version

Article:

Guiastrennec-Faugas, L, Gillet, H, Peakall, J orcid.org/0000-0003-3382-4578 et al. (3 more authors) (2021) Initiation and evolution of knickpoints and their role in cut-and-fill processes in active submarine channels. *Geology*, 49 (3). pp. 314-319. ISSN 0091-7613

<https://doi.org/10.1130/G48369.1>

© 2020 Geological Society of America. This is an author produced version of an article published in *Geology*. Uploaded in accordance with the publisher's self-archiving policy.

Reuse

Items deposited in White Rose Research Online are protected by copyright, with all rights reserved unless indicated otherwise. They may be downloaded and/or printed for private study, or other acts as permitted by national copyright laws. The publisher or other rights holders may allow further reproduction and re-use of the full text version. This is indicated by the licence information on the White Rose Research Online record for the item.

Takedown

If you consider content in White Rose Research Online to be in breach of UK law, please notify us by emailing eprints@whiterose.ac.uk including the URL of the record and the reason for the withdrawal request.



eprints@whiterose.ac.uk
<https://eprints.whiterose.ac.uk/>

1 Initiation and evolution of knickpoints and their role in cut and
2 fill processes in active submarine channels

3 Léa Guiastrennec-Faugas¹, Hervé Gillet¹, Jeff Peakall², Bernard Dennielou³, Arnaud
4 Gaillot³ and Ricardo Silva Jacinto³

5 ¹UMR 5805 EPOC, University of Bordeaux, 33615 PESSAC, France

6 ²School of Earth and Environment, University of Leeds, Leeds LS2 9JT, UK

7 ³IFREMER, Géosciences Marines, 29280 Plouzané, France

8 **ABSTRACT**

9 Submarine channels are the main conduits and intermediate stores for sediment transport into the
10 deep-sea including organics, pollutants, and microplastics. Key drivers of morphological change
11 in channels are upstream migrating knickpoints whose initiation has typically been linked to
12 episodic processes such as avulsion, bend cut-off and tectonics. The initiation of knickpoints in
13 submarine channels has never been described and questions remain about their evolution.
14 Sedimentary and flow processes enabling the maintenance of such features in non-lithified
15 substrates are also poorly documented. Repeated high-resolution multibeam bathymetry between
16 2012-2018 in the Capbreton submarine canyon demonstrates that knickpoints can initiate
17 autogenically at meander bends, over annual to pluri-annual timescales. Partial channel clogging
18 at tight bends is shown to predate the development of new knickpoints. We describe this
19 initiation process and show detailed morphological evolution of knickpoints over time. The
20 gradients of knickpoint headwalls are sustained and can grow over time as they migrate through
21 headward erosion. This morphology, associated plunge pools, and/or development of enhanced
22 downstream erosion are linked herein to the formation and maintenance of hydraulic jumps.

23 These insights of autogenically-driven, temporally high-frequency, knickpoints reveal that cut
24 and fill cycles with depths of multi-meters can be the norm in submarine systems.

25 **INTRODUCTION**

26 Knickpoints are defined as steep steps in channel gradients (Gardner, 1983). They are key drivers
27 of morphological change in submarine channels through controlling phases of channel incision
28 and fill, the formation of terraces, and the development of channel deposit remnants (Heiniö and
29 Davies, 2007; Gales et al., 2019; Turmel et al., 2015; Paull et al., 2011). Knickpoint initiation has
30 been linked to channel avulsion (Deptuck et al., 2007), bend cut-off (Sylvester and Covault,
31 2016) and tectonics (Heiniö and Davies, 2007), however recently, study of an active submarine
32 channel in British Columbia has suggested that knickpoints might be internally generated within
33 channels (Heijnen et al., 2020). Yet we still know surprisingly little about the initiation and
34 evolution of these features. There are key questions on the timescales over which knickpoints
35 form, how they maintain their form in non-lithified substrates, the nature and variability of the
36 flow above them, and consequently their overall influence on sediment transport and deposition.
37 Knickpoint initiation has never been observed in a submarine channel, and the temporal
38 resolution provided by digital elevation models (DEMs) has not allowed the development of
39 knickpoints to be observed in sufficient detail to understand their temporal evolution and
40 associated flow processes. Repeated bathymetric surveys in the Capbreton submarine canyon
41 (CSC) highlight morphological changes over the last 2 decades characterized by upstream
42 knickpoint migration of several 100 m/yr. The surveys were close enough in time to provide a
43 detailed evolution of knickpoints, show how such features of several meters relief are
44 maintained, and enable flow conditions to be inferred. This study shows how knickpoints
45 autogenically initiate and establish a relation with short time scale processes (pluri-annual to

46 annual, seasonal or punctual events such as storms) rather than with long-term processes such as
47 bend cut-off and avulsion (auto- or allogenic) or tectonics (allogenic).

48 **SETTINGS AND DATA**

49 Initiated 50–40 My ago (Ferrer et al., 2008), the CSC lies 300 m offshore at -10 m and extends to
50 -3000 m in the SE of the Bay of Biscay (Fig. 1A). The CSC is nowadays sediment-fed by a
51 southward longshore drift (Mazières et al., 2014). Its former associated river, the Adour, was
52 diverted 15 km southward in 1578 CE (Klingebiel and Legigan, 1978). Water column monitoring
53 by current meters and sediment traps have shown that sediment is transported downcanyon
54 (Mulder et al., 2001; Gaudin et al., 2006; Brocheray et al., 2014) by 2 types of currents: internal
55 tide and low energy turbidity currents ranging from 0.2–0.3 m/s (Mulder et al., 2012). Sediment
56 archives state of recent turbiditic flows with yearly to decadal recurrence over 150 km along the
57 CSC over last 2 kyrs (Mulder et al., 2001; Gaudin et al., 2006; Brocheray et al., 2014).

58 Guiastrennec et al. (2020) described up to 80 knickpoints on the upper CSC floor (-10 to -320
59 m), migrating upstream at rates of 10 m/yr to 1200 m/yr. Here we focus on knickpoint initiation
60 and evolution in three meanders; 2 (M1 & M2) in the upper CSC, at -260 and -300 m (9 & 11 km
61 from the head, along thalweg distance; Figs. 1, 2A, B), and 1 (M3) at -1400 m (90 km from the
62 head; Fig. 1). Five multibeam bathymetric surveys (hull mounted EM2040; grid resolution of 5
63 m) were carried out in spring or summer of 2012, 2013, 2015, 2016 and 2018 over the upper
64 CSC. Real Time Kinematic (RTK) GPS was used for the positioning with a horizontal resolution
65 of 0.01 m and a vertical resolution of 0.02 m; vertical precision < 0.2% of the water depth; tide
66 corrections were made using a tide prediction algorithm from the SHOM (*Service*
67 *Hydrographique et Océanographique de la Marine*); statistics (Guiastrennec et al., 2020)
68 indicate an inter survey bias of just 4 cm with variability of +/-17 cm. Surveys in the upper CSC

69 along with 2 multibeam bathymetric surveys (AUV mounted EM240, grid resolution of 2 m)
70 were also undertaken in 2013 and 2016 in the lower CSC. Positioning resolution < 6 m; vertical
71 precision < 0.5% of the water depth. Inter survey positioning was manually performed based on
72 a nearby area of relatively immobile seabed (Gaillot, 2016).

73 **RESULTS**

74 Time-lapse bathymetry (Figs. 1B, C, 2A, B) show upstream migrating knickpoints both in the
75 shallow (from -260 to -300 m) and deep (-1400 m) parts. Their evolution is controlled by
76 headward erosion and constrained by erosion just downstream of the knickpoint, and deposition
77 further downstream (Figs. 1B, 2A). From 2013 to 2016, knickpoint migration was 706 m/yr in
78 the shallow part, and 190 m/yr in the deep part. Their heights reach 14 m in the deep part and 7
79 m in the shallow part. Plunge pools can be observed at their base respectively up to 10 m deep
80 and < 1 m. (Figs. 1B, C, D, 2C). Straight sections reveal that their headwall slope constantly
81 increased or remained constant: between 2013 and 2018 the headwall slope of knickpoint K1
82 (M3; Fig 1C) gradually increased from 32° to 34° (Fig. 1D) and that of knickpoint K2 (M1 & 2;
83 Fig. 2B) from 5° to 10° (Fig. 2C).

84 In M2 (bend angle ~90°), between 2012 and 2013, the channel became partially blocked at the
85 bend apex by bar deposits leading to the upstream infilling and clogging of the channel (Fig. 2B).
86 3 new knickpoints were observed in 2015 (Fig. 2B) and appear to have been initiated within the
87 meander and were not connected to any other previously present knickpoint downstream of M2.
88 In the 2012 DEM morphological features with vertical relief < 1 m and slopes < 5° are observed
89 downstream of the meander limb but are apparently not genetically related to any knickpoints
90 upstream (Figs. 2A, B).

91 The evolving meander morphology was characterized by a net accumulation of sediment of
92 $\sim 290\text{k m}^3/\text{yr}$ ($\sim 354\text{k m}^3/\text{yr}$ erosion and $\sim 644\text{k m}^3/\text{yr}$ accumulation over respectively ~ 0.41 and
93 $\sim 0.64 \text{ km}^2$) between -300 and -260 m (M1 & 2; Fig. 2A) and $\sim 183\text{k m}^3/\text{yr}$ ($\sim 43\text{k m}^3/\text{yr}$ erosion
94 and $\sim 226\text{k m}^3/\text{yr}$ accumulation over respectively ~ 0.09 and $\sim 0.52 \text{ km}^2$) at -1400 m (M3; Fig.
95 1B). To allow for the different surface areas, volumes have been converted to vertical movement
96 rates (divided by their associated area mention herein above: $\text{m}^3/\text{yr}/\text{m}^2 \rightarrow \text{m}/\text{yr}$; i.e. $644\text{k m}^3/\text{yr} /$
97 $0.64 \text{ km}^2 = 1.01 \text{ m}/\text{yr}$) to obtain $+1.01$ and $-0.87 \text{ m}/\text{yr}$ upstream and $+0.44$ and $-0.50 \text{ m}/\text{yr}$
98 downstream. Knickpoint migration rate and budget sediment accumulation are higher in the 2
99 shallower meanders (M1 & 2) than in the deepest meander (M3).

100 **DISCUSSION**

101 **Knickpoint initiation**

102 We interpret these morphologic changes as showing knickpoints initiating at meanders with
103 acute angles prone to point-bar sediment accumulation in the channel. Previous flume work
104 revealed that high bend angles allow sediment to deposit just upstream of the bend apex, such as
105 point bars in rivers (Peakall et al., 2007). We observe repetition of 2 knickpoints and bars along
106 the channel (Fig. 2), with up to 9 repetitions in the adjacent canyon (Guiastrennec et al., 2020).
107 The sediment eroded by knickpoint upstream migration is mobilised and bypassed down system,
108 and bar formation occurs downstream (Fig. 2B). At the sharp bend, bar formation is enhanced as
109 observed in fluvial environments. At this point, we assume that the clogging of the channel (i.e.
110 M2; Figs. 3A, B) confines the flow and increases tortuosity of flow around the bend, spreading
111 and/or focusing flow onto the bar. As flow reconnected with the deeper channel downstream, it
112 led to backstepping erosion of the point bar deposit in the form of three chute channels (Figs. 3C,
113 D). Flow thickness will have reduced over the point bar potentially leading to supercritical flow

114 (Froude number >1). At the downstream end of the bar, flow will then undergo rapid deepening
115 as it reconnects with the deeper main channel, in which case the flow will likely become
116 subcritical, and a hydraulic jump may have been generated at the transition. The bar also laterally
117 confines the thalweg likely inducing flow acceleration and therefore promoting supercritical
118 conditions, and hence the thalweg might be expected to develop chute channels. However, in this
119 case a topographic step (bar-thalweg transition) with its associated gradient appears needed to
120 create flow conditions required to initiate knickpoints.

121 M2 and M3 both present a shallow upstream meander limb, compared to downstream of the bend
122 apex. These similar morphologies combined with the occurrence of chute channels (Figs. 2C, D,
123 3F, G) suggests similar processes in both meanders. In M1, with a bend angle $\sim 160^\circ$, yearly
124 time-lapse morphology reveals that a point bar did not develop, illustrating the likely different
125 flow conditions associated with large bend angles.

126 Here, the cut and fill behavior related to knickpoints takes place without involvement of major
127 external factors, tectonics or avulsion. No major slump scars are evidenced on the canyon flanks
128 (Guiastrennec et al., 2020). Neither water depth, or the rate of sediment accumulation, seem to
129 control knickpoint initiation. Thus, it is the combination of a sharp bend, and sediment
130 accumulation supplied from the process of knickpoint migration (erosion and then deposition),
131 that leads to the autogenic initiation of knickpoints. As new knickpoints migrate upstream, this
132 results in repeated channel clogging (bar formation) and the subsequent development of a new
133 knickpoint. Essentially, each knickpoint generates the next one.

134 Point-bar development, and bend cut-off (Sylvester and Covault, 2016), are both autogenic
135 processes for the generation of knickpoints, associated with channel evolution and migration.

136 Nevertheless, evolution in the CSC is observed in an already established canyon and migration

137 only affects the axial channel, while in the study of Sylvester and Covault (2016) knickpoint
138 initiation is linked to migration of the entire channel.

139 **Knickpoint evolution and flow conditions**

140 Erosion initiated on the point-bar (M2) continues along the canyon thalweg in the form of
141 knickpoint upstream migration (i.e. K2 on Fig. 2; Fig. 3E). Morphology time-lapse confirms that
142 incipient knickpoints are gentle steps that become steeper, as they migrate upstream (Fig. 2).
143 The observation of plunge pools is evidence of the presence of hydraulic jumps (Komar, 1971;
144 Bourget et al., 2011; Mulder et al., 2019). Hydraulic jumps imply a shift from supercritical to
145 subcritical flow conditions, and thus imply that such flow conditions can be related to
146 knickpoints (Fig. 4). Previous laboratory experiments on non-indurated sediments (simulating
147 river alluvial beds) confirm highly variable flow conditions in the vicinity of knickpoints
148 (Toniolo and Cantelli, 2007). Measurements of subaqueous hydraulic jumps over scours in the
149 Black Sea (Dorrell et al., 2016) show flow acceleration on the headwall. The hydraulic jump will
150 lead to erosion at the base of the slope resulting in an area of nondeposition/erosion representing
151 sediment mobilized/excavated by the hydraulic jump just downstream of the knickpoints
152 (Mitchell, 2006). In the CSC, plunge pools are not systematically observed downstream of
153 knickpoints but areas of erosion are. In either case, knickpoints develop where depth suddenly
154 increases (bar-thalweg transition), which may encourage a hydraulic jump.
155 Two cores sampled in the study area at -301 m (thalweg) and -251 m (terrace) have recorded
156 very coarse sand and gravel in the thalweg and a continuous silty-clay deposit on the terrace, 50
157 m above the thalweg (Duros et al., 2017). A third core located upstream on a terrace, at -214 m
158 and 13 m above the thalweg, sampled medium-sand turbidites (Guiastrennec et al., 2020). The
159 grain-size variations suggest that flows are highly stratified, with the sand-rich component at

160 least 13 m thick, but less than 50 m. The knickpoint relief (up to 7 m) is therefore relatively small
161 compared to total estimated flow thickness, however the stratified nature of the flow, and the
162 coupling of velocity and sediment, mean that momentum is highly concentrated towards the base
163 of stratified sand-rich turbidity currents (Wells and Dorrell, 2021). The basal parts would be
164 expected to respond to the increased gradients across knickpoints (Dorrell et al., 2016).
165 Erosion areas, including plunge pools, are crucial to the sustainability of knickpoints and their
166 migration and directly depend on flow dynamics. Erosion against the headwall maintains a local
167 steep slope. In turn, the steep gradient promotes hydraulic jumps at that location, which
168 propagates the knickpoint structure (Fig. 4). Erosion on top of the headwall could either be
169 related to flow characteristics (erosion at the base of flow), or be related to a collapse as a
170 consequence of erosion at the base of the headwall as suggested by Heijnen et al. (2020), or both.
171 At -1400 m, the lower velocity of knickpoint migration and sediment accumulation budget in
172 comparison to the 2 shallower meanders suggest less frequent flows. This is consistent with
173 observations made in Monterey Canyon (Stevens et al., 2014) where turbidity current activity
174 (number and intensity) decreases with the distance from the source. The type and size of
175 turbidity currents (volume and sediment concentration with regard to channel floor dimension)
176 could determine the occurrence of plunge pools and the sustainability and migration of
177 knickpoints. The highest knickpoints and the deepest plunge pools are found in the deeper
178 section, and exhibit slower upstream migration, perhaps related to the lower positive sediment
179 budget whose consequence would be a better morphological expression and preservation of
180 erosional processes and features.

181 **CONCLUSION**

182 Using high-resolution repeated bathymetry from the CSC we identify autogenic initiation of
183 knickpoints for the first time, reveal the morphological evolution of knickpoints, and link the
184 morphology to the formation and maintenance of hydraulic jumps. The combination of sediment
185 supply and meander morphology leading to point bar deposition and channel clogging is
186 observed to be among the possible prerequisites for knickpoint initiation. This data reveals that
187 knickpoints in non-lithified substrates can initiate and develop autogenically on annual and
188 maybe seasonal and event time scales, orders of magnitude shorter than the periodicity envisaged
189 from mechanisms such as avulsion, tectonism, and bend cut-off. We demonstrate that cut and fill
190 cycles with depths of multi-meters, driven by high-frequency autogenic knickpoints, can be the
191 norm in submarine systems capable of supporting flows with velocities sufficient to create
192 hydraulic jumps. Thus, the observation of large-scale (multi-meter) erosion surfaces in
193 channelized submarine systems in the rock record can be autogenic and geologically
194 instantaneous and do not imply changes in external controls, nor temporal scales beyond multi-
195 annual.

196 **ACKNOWLEDGEMENTS**

197 We thank IFREMER, the SHOM and all the cruise parties and crews for their assistance. We also
198 thank RTE for the permission to use data from the Volt program and cruises. We thank the
199 French Ministry MESRI for the grant. We thank N. Mitchell, C. Stevenson and an anonymous
200 reviewer, along with editor J. Schmitt, for their thorough and constructive reviews that have
201 greatly improved the paper.

202 Fig. 1: (A) Location of the study area in the Bay of Biscay; (B, C, D) Meander 3 evolution
203 between 2013 and 2016; (B) Elevation change suggesting erosion and deposition. (C) Elevation

204 relative to mean thalweg longitudinal profile. (D) In grey, longitudinal profile of K1; black line:
205 along-profile slope magnitude; blue area highlights plunge pools.

206 Fig. 2: Meander 1 & 2 (loc. on Fig. 1A) evolution through years 2012, 2013, 2015, 2016 and
207 2018, parts A to C as per Figures 1B-1D.

208 Fig. 3: Knickpoint initiation on a bar deposit in a meander-bend based on the cases of M2 & 3.

209 (A, B) In M2, bar expansion leads to the clogging of the channel, shallowing the upstream

210 meander limb; (C, D) Backstepping erosion of the bar and knickpoint upstream migration in

211 form of three chute channels. (E) Erosion on the bar and knickpoint migration continues along

212 the canyon thalweg. (F, G) M3 presents a shallow upstream meander limb and the occurrence of

213 knickpoints and chute channels.

214 Fig. 4: Schematic longitudinal sketch of flow conditions and temporal evolution of a knickpoint

215 and associated plunge pool. Knickpoint upstream migration occurs by erosion of the headwall.

216 Erosion at the base of the headwall sustains the knickpoint slope whilst moving sediment further

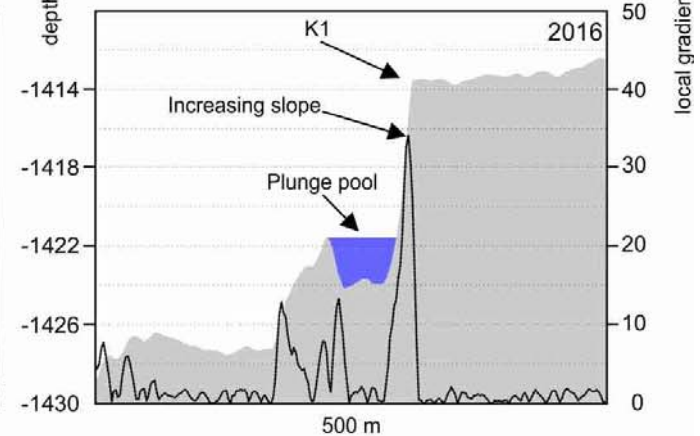
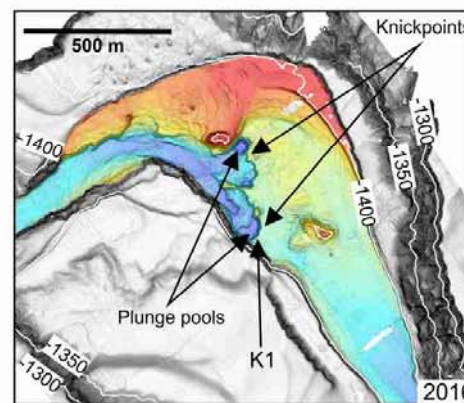
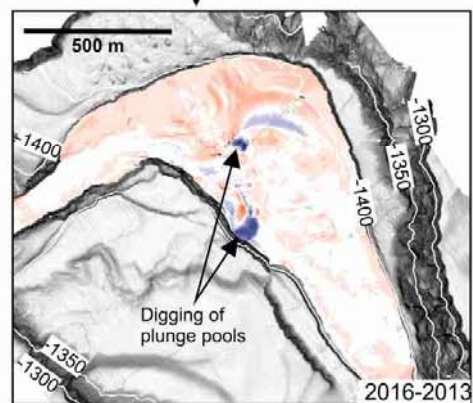
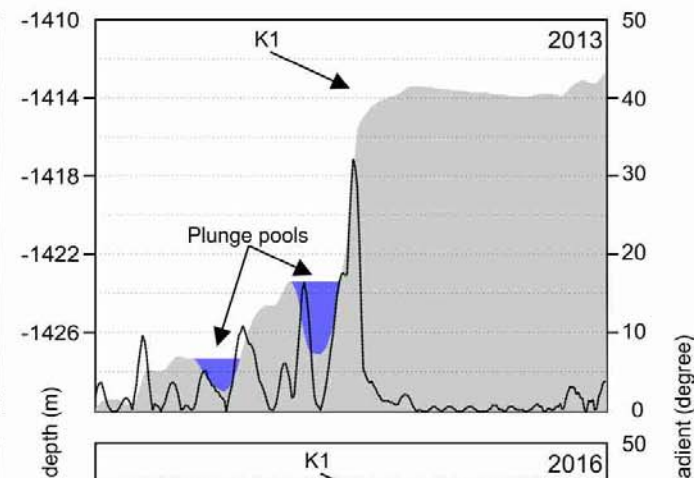
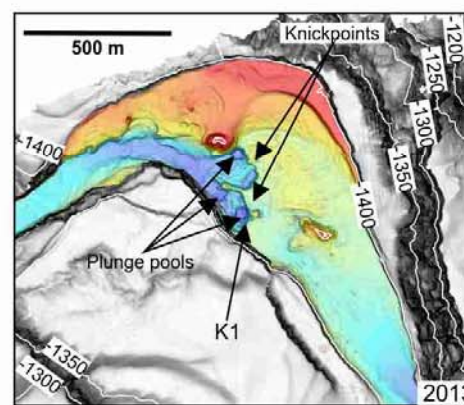
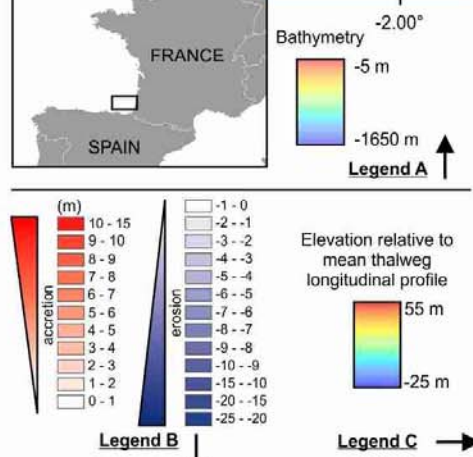
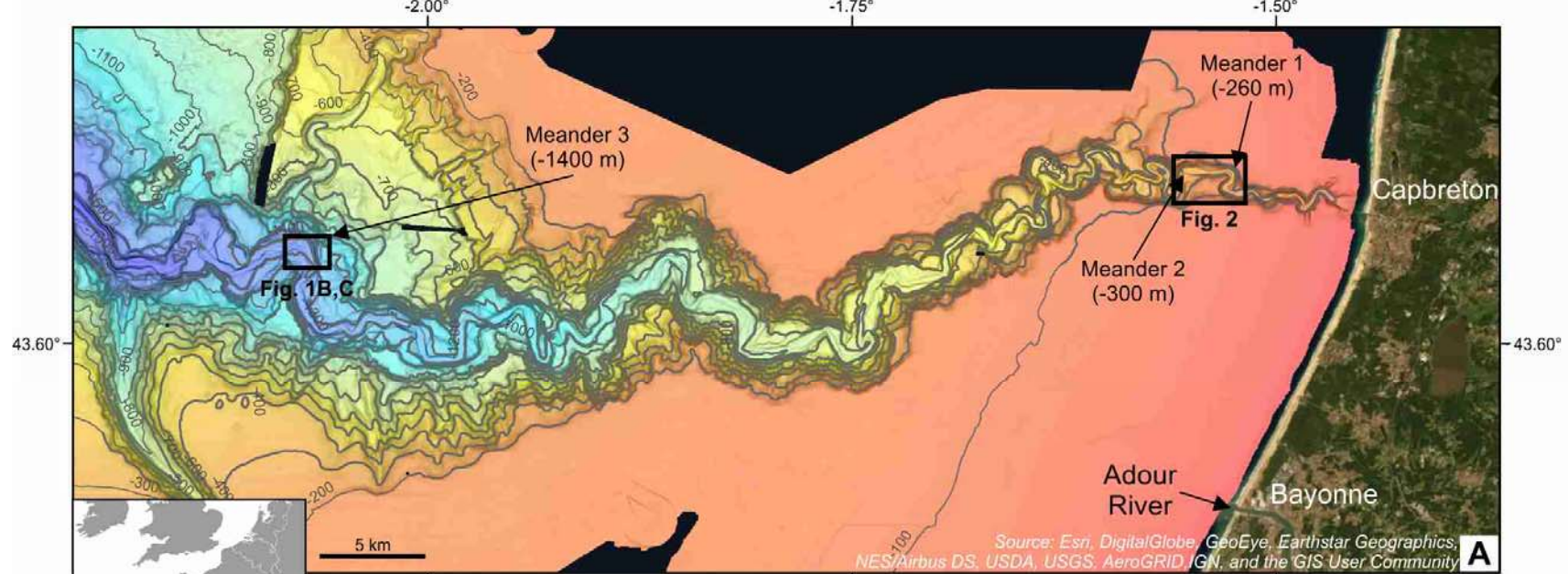
217 downdip, where sedimentation forms a new bar.

218 REFERENCES CITED

- 219 Bourget, J., Zaragosi, S., Ellouz-Zimmermann, N., Mouchot, N., Garlan, T., Schneider, J.-L.,
220 Lanfumey, V., Lallemand, S., 2011. Turbidite system architecture and sedimentary processes
221 along topographically complex slopes: the Makran convergent margin: The Makran turbidite
222 system. *Sedimentology* 58, 376–406. <https://doi.org/10.1111/j.1365-3091.2010.01168.x>
223 Brocheray, S., Cremer, M., Zaragosi, S., Schmidt, S., Eynaud, F., Rossignol, L., Gillet, H., 2014.
224 2000years of frequent turbidite activity in the Capbreton Canyon (Bay of Biscay). *Mar. Geol.*
225 347, 136–152. <https://doi.org/10.1016/j.margeo.2013.11.009>
226 Deptuck, M.E., Sylvester, Z., Pirmez, C., O’Byrne, C., 2007. Migration–aggradation history and
227 3-D seismic geomorphology of submarine channels in the Pleistocene Benin-major Canyon,
228 western Niger Delta slope. *Mar. Pet. Geol.* 24, 406–433.
229 <https://doi.org/10.1016/j.marpetgeo.2007.01.005>
230 Dorrell, R.M., Peakall, J., Sumner, E.J., Parsons, D.R., Darby, S.E., Wynn, R.B., Özsoy, E.,
231 Tezcan, D., 2016. Flow dynamics and mixing processes in hydraulic jump arrays: Implications
232 for channel-lobe transition zones. *Mar. Geol.* 381, 181–193.
233 <https://doi.org/10.1016/j.margeo.2016.09.009>
234 Duros, P., Silva Jacinto, R., Dennielou, B., Schmidt, S., Martinez Lamas, R., Gautier, E., Roubi,
235 A., Gayet, N., 2017. Benthic foraminiferal response to sedimentary disturbance in the Capbreton
236 canyon (Bay of Biscay, NE Atlantic). *Deep Sea Res. Part Oceanogr. Res. Pap.* 120, 61–75.
237 <https://doi.org/10.1016/j.dsr.2016.11.012>
238 Ferrer, O., Roca, E., Benjumea, B., Muñoz, J.A., Ellouz, N., MARCONI Team, 2008. The deep
239 seismic reflection MARCONI-3 profile: Role of extensional Mesozoic structure during the
240 Pyrenean contractional deformation at the eastern part of the Bay of Biscay. *Mar. Pet. Geol.* 25,
241 714–730. <https://doi.org/10.1016/j.marpetgeo.2008.06.002>
242 Gales, J.A., Talling, P.J., Cartigny, M.J.B., Hughes Clarke, J., Lintern, G., Stacey, C., Clare,
243 M.A., 2019. What controls submarine channel development and the morphology of deltas
244 entering deep-water fjords? *Earth Surf. Process. Landf.* 44, 535–551.
245 <https://doi.org/10.1002/esp.4515>
246 Gaillot Arnaud (2016). VOLT2. Interconnexion électrique France-Espagne.
247 Traitement des données SMF EM2040 AUV Différentiel bathymétrique
248 2013-2016. N/O Thalassa du 20/07 au 26/07 2016 . DIT.REM/GM/CTDI
249 20161020-AG01. Gamberi, F., Breda, A., Mellere, D., 2017. Depositional canyon heads at the
250 edge of narrow and tectonically steepened continental shelves: Comparing geomorphic elements,
251 processes and facies in modern and outcrop examples. *Mar. Pet. Geol.* 87, 157–170.
252 <https://doi.org/10.1016/j.marpetgeo.2017.06.007>
253 Gardner, T.W., 1983. Experimental study of knickpoint and longitudinal profile evolution in
254 cohesive, homogeneous material. *GSA Bull.* 94, 664–672. [https://doi.org/10.1130/0016-7606\(1983\)94<664:ESOKAL>2.0.CO;2](https://doi.org/10.1130/0016-7606(1983)94<664:ESOKAL>2.0.CO;2)
255
256 Gaudin, M., Mulder, T., Cirac, P., Berné, S., Imbert, P., 2006. Past and present sedimentary
257 activity in the Capbreton Canyon, southern Bay of Biscay. *Geo-Mar. Lett.* 26, 331–345.
258 <https://doi.org/10.1007/s00367-006-0043-1>
259 Guiastrennec-Faugas, L., Gillet, H., Jacinto, R.S., Dennielou, B., Hanquiez, V., Schmidt, S.,
260 Simplet, L., Rousset, A., 2020. Upstream migrating knickpoints and related sedimentary
261 processes in a submarine canyon from a rare 20-year morphobathymetric time-lapse (Capbreton

262 submarine canyon, Bay of Biscay, France). *Mar. Geol.* 106143.
263 <https://doi.org/10.1016/j.margeo.2020.106143>
264 Heijnen, M.S., Clare, M.A., Cartigny, M.J.B., Talling, P.J., Hage, S., Lintern, D.G., Stacey, C.,
265 Parsons, D.R., Simmons, S.M., Chen, Y., Sumner, E.J., Dix, J.K., Hughes Clarke, J.E., 2020.
266 Rapidly-migrating and internally-generated knickpoints can control submarine channel
267 evolution. *Nat. Commun.* 11. <https://doi.org/10.1038/s41467-020-16861-x>
268 Heiniö, P., Davies, R.J., 2007. Knickpoint migration in submarine channels in response to fold
269 growth, western Niger Delta. *Mar. Pet. Geol.* 24, 434–449.
270 <https://doi.org/10.1016/j.marpetgeo.2006.09.002>
271 Klingebiel, A., Legigan, P., 1978. Histoire géologique des divagations de l'Adour Proc Congr
272 IVème Centenaire du Détournement de l'Adour 1578–1978, Bayonne.
273 Komar, P.D., 1971. Hydraulic Jumps in Turbidity Currents. *Geol. Soc. Am. Bull.* 82, 1477.
274 [https://doi.org/10.1130/0016-7606\(1971\)82\[1477:HJITC\]2.0.CO;2](https://doi.org/10.1130/0016-7606(1971)82[1477:HJITC]2.0.CO;2)
275 Mazières, A., Gillet, H., Castelle, B., Mulder, T., Guyot, C., Garlan, T., Mallet, C., 2014. High-
276 resolution morphobathymetric analysis and evolution of Capbreton submarine canyon head
277 (Southeast Bay of Biscay—French Atlantic Coast) over the last decade using descriptive and
278 numerical modeling. *Mar. Geol.* 351, 1–12. <https://doi.org/10.1016/j.margeo.2014.03.001>
279 Mitchell, N.C., 2006. Morphologies of knickpoints in submarine canyons. *Geol. Soc. Am. Bull.*
280 17.
281 Mulder, T., Gillet, H., Hanquiez, V., Reijmer, J.J.G., Droxler, A.W., Recouvreur, A., Fabregas, N.,
282 Cavailhes, T., Fauquembergue, K., Blank, D.G., Guaiastrennec, L., Seibert, C., Bashah, S., Bujan,
283 S., Ducassou, E., Principaud, M., Conesa, G., Le Goff, J., Ragusa, J., Busson, J., Borgomano, J.,
284 2019. Into the deep: A coarse-grained carbonate turbidite valley and canyon in ultra-deep
285 carbonate setting. *Mar. Geol.* 407, 316–333. <https://doi.org/10.1016/j.margeo.2018.11.003>
286 Mulder, T., Weber, O., Anschutz, P., Jorissen, F., Jouanneau, J.-M., 2001. A few months-old
287 storm-generated turbidite deposited in the Capbreton Canyon (Bay of Biscay, SW France). *Geo-*
288 *Mar. Lett.* 21, 149–156. <https://doi.org/10.1007/s003670100077>
289 Mulder, T., Zaragosi, S., Garlan, T., Mavel, J., Cremer, M., Sottolichio, A., Sénéchal, N.,
290 Schmidt, S., 2012. Present deep-submarine canyons activity in the Bay of Biscay (NE Atlantic).
291 *Mar. Geol.* 295–298, 113–127. <https://doi.org/10.1016/j.margeo.2011.12.005>
292 Paull, C.K., Caress, D.W., Iii, W.U., Lundsten, E., Meiner-Johnson, M., 2011. High-resolution
293 bathymetry of the axial channels within Monterey and Soquel submarine canyons, offshore
294 central California 25. <https://doi.org/10.1130/GES00636.1>
295 Peakall, J., Ashworth, P.J., Best, J.L., 2007. Meander-Bend Evolution, Alluvial Architecture, and
296 the Role of Cohesion in Sinuous River Channels: A Flume Study. *J. Sediment. Res.* 77, 197–212.
297 <https://doi.org/10.2110/jsr.2007.017>
298 Stevens, T., Paull, C.K., Ussler, W., III, McGann, M., Buylaert, J.-P., Lundsten, E., 2014. The
299 timing of sediment transport down Monterey Submarine Canyon, offshore California. *GSA Bull.*
300 126, 103–121. <https://doi.org/10.1130/B30931.1>
301 Sylvester, Z., Covault, J.A., 2016. Development of cutoff-related knickpoints during early
302 evolution of submarine channels. *Geology* 44, 835–838. <https://doi.org/10.1130/G38397.1>
303 Toniolo, H., Cantelli, A., 2007. Experiments on Upstream-Migrating Submarine Knickpoints. *J.*
304 *Sediment. Res.* 77, 772–783. <https://doi.org/10.2110/jsr.2007.067>
305 Turmel, D., Locat, J., Parker, G., 2015. Morphological evolution of a well-constrained, subaerial-
306 subaqueous source to sink system: Wabush Lake. *Sedimentology* 62, 1636–1664.
307 <https://doi.org/10.1111/sed.12197>

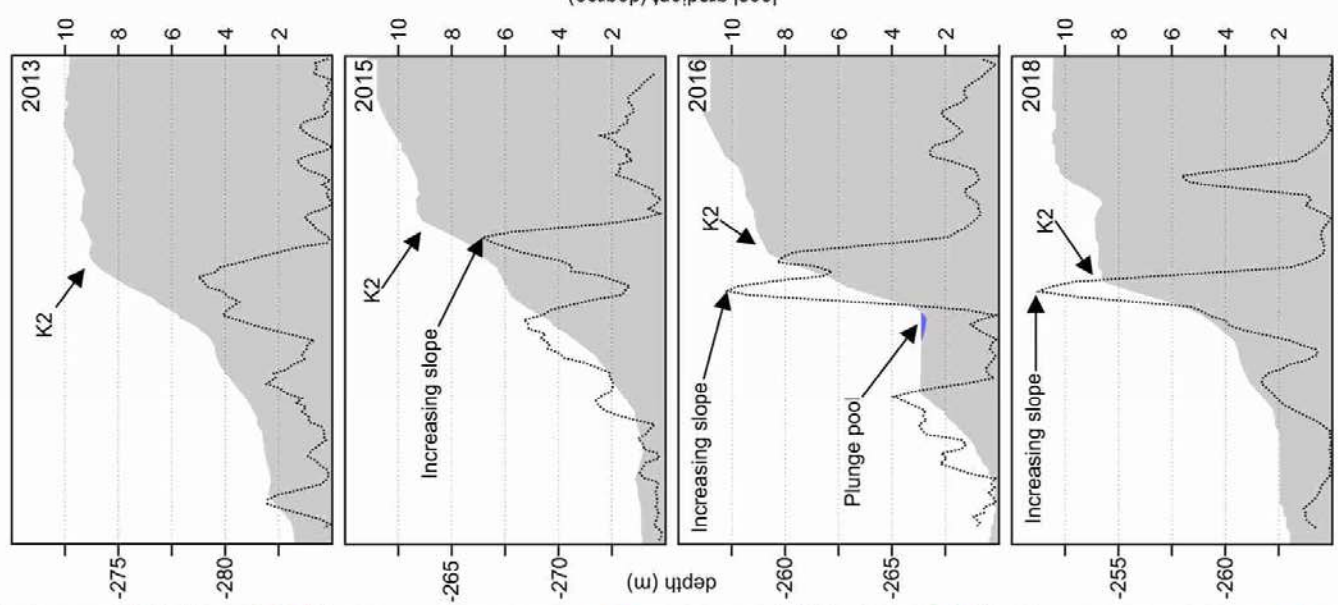
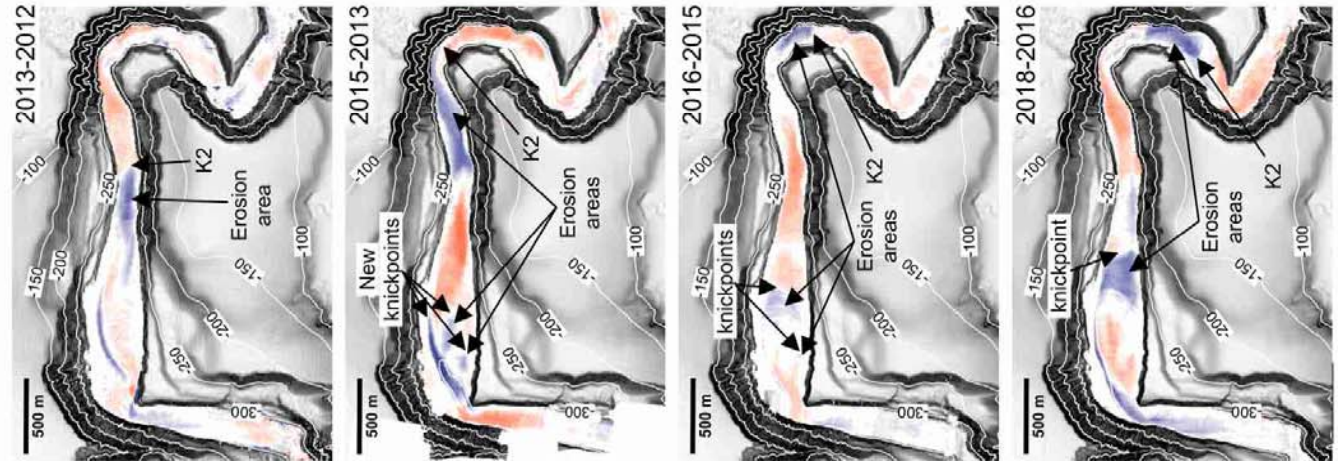
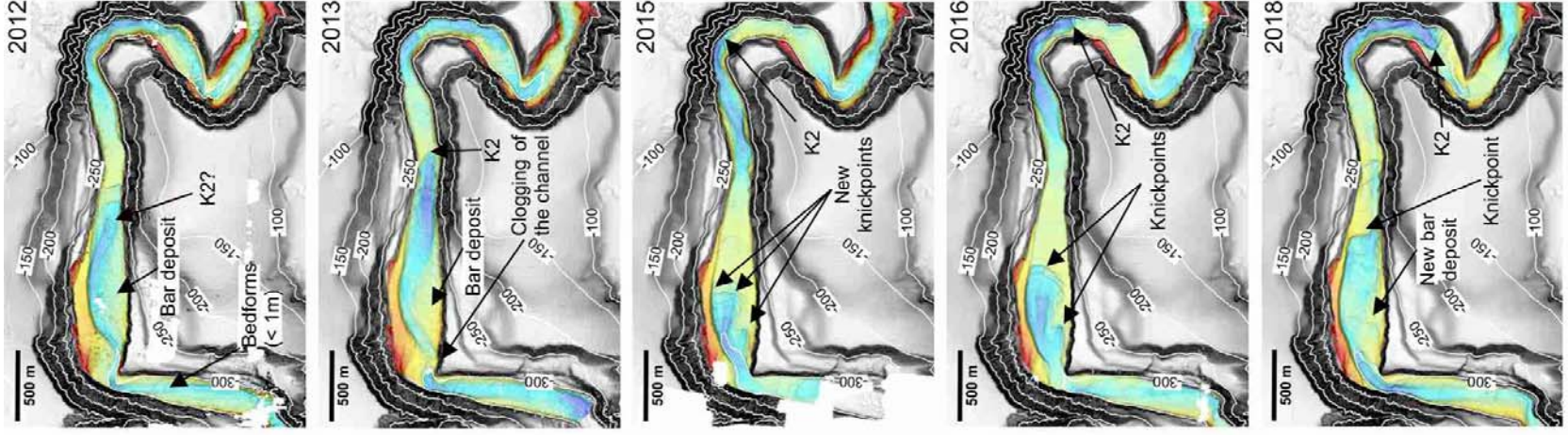
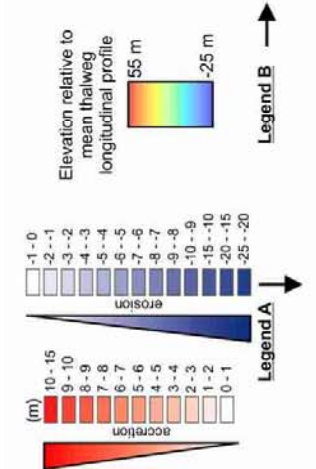
308 Wells, M.G., Dorrell, R.M., 2021. Turbulence processes within turbidity currents. Annual
309 Review of Fluid Mechanics 53, 59-83.
310



B

C

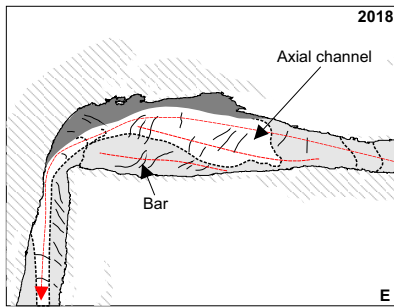
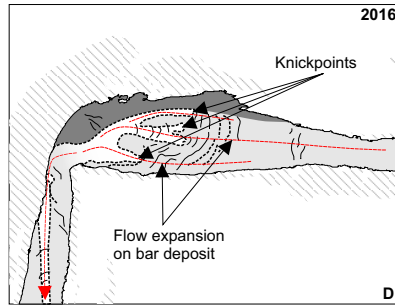
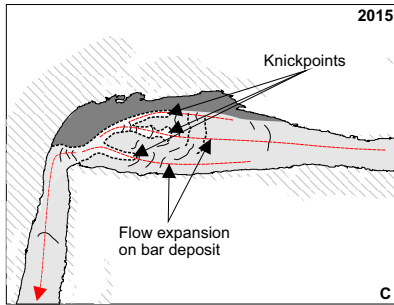
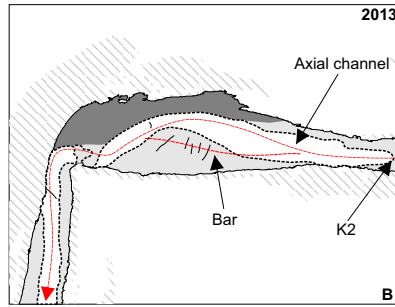
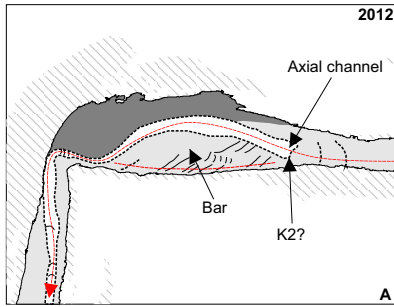
D



B

A

400 m
C



Legend:

- | | |
|-----------------------------|-------------------------------|
| Inter-channel sedimentation | Channel incision |
| Low terrace level | Rocky outcrops |
| High terrace level | Bedforms |
| Plunge pool | Knickpoint |
| Steep flanks | Suggested main flow direction |

